INTERNATIONAL JOURNAL FOR NUMERICAL METHODS IN FLUIDS, VOL. 12, 859–879 (1991)

DYNAMICS OF LIQUID MEMBRANES. I: NON-ADAPTIVE FINITE DIFFERENCE METHODS

J. I. RAMOS*

F. Informática/ETSI Telecomunicación, Universidad de Málaga, Plaza El Ejido, E-29013 Málaga, Spain

AND

R. PITCHUMANI

Department of Mechanical Engineering, Carnegie-Mellon University, Pittsburgh, PA 15213-3890, U.S.A.

SUMMARY

A non-adaptive method and a Lagrangian–Eulerian finite difference technique are used to analyse the dynamic response of liquid membranes to imposed pressure variations. The non-adaptive method employs a fixed grid and upwind differences for the convection terms, whereas the Lagrangian–Eulerian technique uses operator splitting and decomposes the mixed convection–diffusion system of equations into a sequence of convection and diffusion operators. The convection operator is solved exactly by means of the method of characteristics, and its results are interpolated onto the fixed (Eulerian) grid used to solve the diffusion operator. It is shown that although the method of characteristics eliminates the numerical diffusion associated with upwinding the convection terms in a fixed Eulerian grid, the Lagrangian–Eulerian method may yield overshoots and undershoots near steep flow gradients or when rapid pressure gradients are imposed, owing to the interpolation of the results of the convection operator onto the fixed grid used to solve the diffusion operator. This interpolation should be monotonic and positivity-preserving and should satisfy conservation of mass and linear momentum. It is also shown that both the non-adaptive and Lagrangian–Eulerian finite difference methods produce almost identical (within 1%) results when liquid membranes are subjected to positive and negative step and ramp changes in the pressure coefficient. However, because of their non-adaptive character, these techniques require an estimate of the (unknown) length of the membrane and do not use all the grid points in the calculations. The liquid membrane dynamic response is also analysed as a function of the Froude number, convergence parameter and nozzle exit angle for positive and negative step and ramp changes in the pressure coefficient.

KEY WORDS Liquid membranes Lagrangian–Eulerian finite difference methods

INTRODUCTION

Vertical annular liquid jets or liquid curtains have applications as protection systems for inertial confinement laser fusion (ICF) reactors and as chemical reactors.[1] Cylindrical chemical reactors can be used for stack emission scrubbing for pollution control, reaction and control of toxic wastes and scrubbing of radioactive and non-radioactive particulates and soluble materials.[1]

Ramos[2] derived the equations governing the dynamics of axisymmetric liquid curtains and axisymmetric liquid membranes from Cauchy's equations and obtained analytical solutions for

* On leave from Department of Mechanical Engineering, Carnegie–Mellon University, Pittsburgh, PA 15213–3890, U.S.A.

0271–2091/91/090859–21$10.50 *Received 4 September 1989*

steady state, inviscid, long liquid curtains and liquid membranes as a function of the Froude and Weber numbers, nozzle exit angle and pressure difference across liquid curtains and liquid membranes.[1,2] Ramos and Pitchumani[3,4] solved the equations governing the dynamics of liquid curtains and liquid membranes using a non-adaptive finite difference method and obtained numerical solutions as a function of the liquid curtain and liquid membrane parameters.

In this paper the dynamics of liquid membranes is analysed by means of two non-adaptive finite difference methods. One of the methods is based on the direct discretization of the governing convection–diffusion equations, whereas the other method uses operator splitting to decompose the mixed convection–diffusion operators into a sequence of convection and diffusion operators. The convection operators are solved by means of the method of characteristics, i.e. a Lagrangian approach is employed, and their results are interpolated onto the fixed (Eulerian) grid used to solve the diffusion operators. The objective of this operator-splitting procedure is to minimize the numerical diffusion which arises when the convection operators are solved in a fixed grid, and since the method uses the method of characteristics and a fixed grid, it will be referred to as a characteristic–finite difference or Lagrangian–Eulerian procedure.

The equations governing the dynamics of liquid membranes[2] are presented in the second section, while the numerical methods used to solve the governing partial differential equations are presented in the third section. The fourth and fifth sections of this paper deal with the presentation of results and conclusions respectively.

PROBLEM FORMULATION

Consider the axisymmetric, vertical liquid membrane shown in Figure 1 and assume that the liquid is isothermal and incompressible. If the friction forces on the gases surrounding ($r > R$)

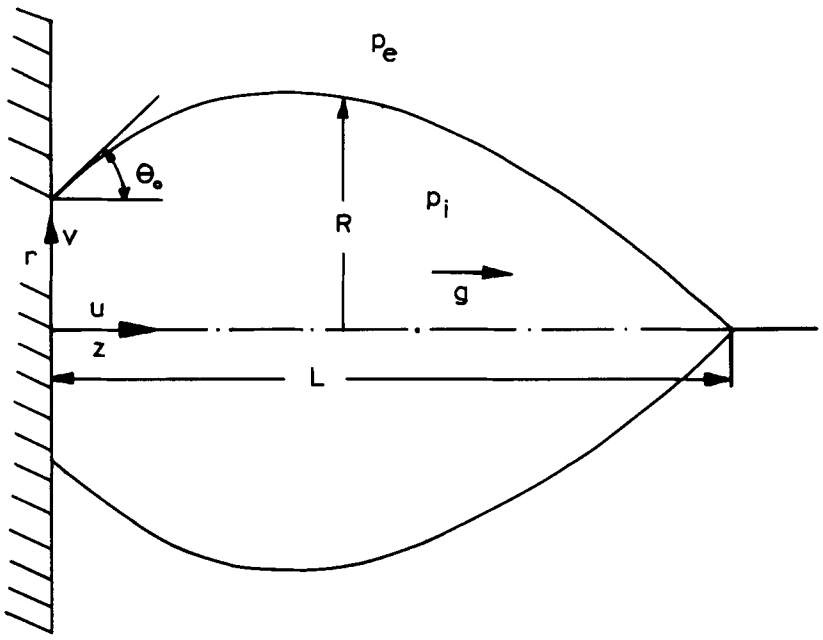

Figure 1. Schematic of a liquid membrane

and enclosed ($r < R$) by the liquid membrane are negligible, and if the liquid is inviscid, the equations governing the dynamics of axisymmetric, vertical liquid membranes can be written as[2] ($t > 0, 0 < z < L(t)$)

$$\frac{\partial m}{\partial t} + \frac{\partial}{\partial z}(mu) = 0, \tag{1}$$

$$\frac{\partial}{\partial t}(mu) + \frac{\partial}{\partial z}(muu) = mg + \left(\frac{2\sigma J'}{RR'} + (p_e - p_i)\right) RR', \tag{2}$$

$$\frac{\partial}{\partial t}(mv) + \frac{\partial}{\partial z}(muv) = -\left(\frac{2\sigma J'}{RR'} + (p_e - p_i)\right) R, \tag{3}$$

$$v = \frac{\partial R}{\partial t} + u\frac{\partial R}{\partial z}, \tag{4}$$

where m is the mass per unit length per radian of the liquid membrane, u and v are the axial and radial velocity components respectively, t is time, z is the axial co-ordinate, g is the gravitational acceleration, σ is the surface tension, p_i and p_e are the pressures of the gases enclosed by and surrounding the liquid membrane respectively, $R = R(t, z)$ is the instantaneous local radius of the liquid membrane, L is the liquid membrane convergence length (Figure 1), the primes denote differentiation with respect to z and

$$J = R \Big/ \left[1 + \left(\frac{\partial R}{\partial z}\right)^2\right]^{1/2}. \tag{5}$$

Equations (1)–(3) represent mass and linear momentum conservation in the axial and radial directions respectively, while equation (4) corresponds to the kinematic condition at the liquid membrane.

In order to understand the effects of different variables on the dynamic response of liquid membranes, it is necessary to introduce the following dimensionless quantities:

$$R^* = \frac{R}{R_0}, \quad z^* = \frac{z}{R_0}, \quad u^* = \frac{uu_0}{gR_0}, \quad v^* = \frac{vu_0}{gR_0}, \quad C_{pn} = (p_i - p_e)\frac{R_0}{2\sigma}, \tag{6}$$

$$\tau = \frac{gt}{u_0}, \quad We = \frac{m_0 u_0^2}{2\sigma R_0}, \quad Fr = \frac{u_0^2}{gR_0}, \quad N = \frac{We}{Fr^2}, \tag{7}$$

$$m^* = \frac{m}{m_0}, \quad M^* = m^*u^*, \quad N^* = m^*v^*, \quad R_1^* = m^*R^*, \tag{8}$$

where R_0, u_0 and m_0 denote the liquid membrane radius, axial velocity and mass per unit length per radian at the nozzle exit, i.e. at $z = 0$, respectively, Fr and We are the Froude and Weber numbers respectively, N is the convergence parameter and M^* and N^* are the non-dimensional linear momentum per unit length and per radian in the axial and radial directions respectively.

Substitution of equations (6)–(8) into equations (1)–(4) yields the following system of equations:

$$\frac{\partial \mathbf{U}}{\partial \tau} + \frac{\partial \mathbf{F}}{\partial z^*} = \mathbf{G}, \tag{9}$$

where

$$\mathbf{U} = (m^*, R_1^*, M^*, N^*)^T, \tag{10}$$

$$\mathbf{F} = [M^*, R_1^* M^*/m^*, M^{*2}/m^*, M^* N^*/m^*]^T, \tag{11}$$

$$\mathbf{G} = [0, N^*, Frm^* - (C_{pn} R^* R^{*\prime} - J^{*\prime})/N, (-J^{*\prime}/R^{*\prime} + C_{pn} R^*)/N]^T \tag{12}$$

and, the superscript T denotes transpose.

Equation (9) is subject to the following boundary condition:

$$\mathbf{U}(\tau, z^* = 0) = (1, 1, 1, \tan\theta_0)^T, \tag{13}$$

where θ_0 denotes the nozzle exit angle (Figure 1). The initial conditions will be specified in the section on the 'Presentation of results'.

Note that the right-hand-sides of equations (2) and (3) contain $R'' = \partial^2 R/\partial z^2$ and therefore equation (9) represents a mixed, non-linear convection–diffusion problem. Furthermore, while the pressure p_e of the gases surrounding the liquid membrane may be assumed constant, the pressure p_i of the gases enclosed by the liquid membrane is determined, in the absence of mass leakage and mass dissolution by the volume enclosed by the membrane, as follows. If the gases enclosed by the membrane are assumed to be isothermal and ideal, then

$$p_i = \rho_i \tilde{R} T, \tag{14}$$

where ρ_i denotes the density of the gases enclosed by the membrane, $\tilde{R}$ is specific gas constant and T is the temperature. In the absence of chemical reaction and mass dissolution and leakage, equation (14) can be integrated to yield

$$p_i = m_i \tilde{R} T \Big/ \left(\pi \int_0^L R^2 \, dz \right), \tag{15}$$

where m_i is the (constant) mass of the gases enclosed by the liquid membrane and L is the convergence length defined as the axial location at which $R(L, t) = 0$.

Equations (2), (3) and (15) clearly indicate that equation (9) represents an integrodifferential convection–diffusion system. In this paper we shall be concerned with equation (9) and a specified pressure of the gases enclosed by the liquid membrane, i.e. p_i, and therefore C_{pn} will be specified as a function of time. This problem will be referred to as a direct problem since p_i is specified as a function of time and is related to forced distributed parameter systems. The dependence of the pressure coefficient C_{pn} on the non-dimensional time τ, i.e. $C_{pn} = C_{pn}(\tau)$, will be presented in the section on the 'Presentation of results'.

Direct problems can be realized in practice if the gases enclosed by the liquid membrane undergo an isothermal chemical reaction where the number of moles of the combustion products is different from that of the reactants. If the characteristic chemical reaction time is much shorter than the hydrodynamic timescales of the liquid membrane, it can be assumed that the reaction is instantaneous and C_{pn} changes instantaneously, i.e. it suffers a jump. This jump may be positive or negative depending on whether the number of moles of the combustion products is larger or smaller than that of the reactants.

The isothermal reactions of the gases enclosed by the liquid membrane may also occur in a finite time or may possess a cyclic behaviour characterized by periodic pressure variations. In this paper we will consider both instantaneous and smooth changes in the pressure coefficient corresponding to instantaneous and finite rate chemical reactions in the gases enclosed by the liquid curtain, whereas in Part II we will consider cyclic reactions which result in periodic pressure variations.

NUMERICAL METHODS

Equation (9) with $C_{pn} = C_{pn}(\tau)$ represents a forced system of mixed convection–diffusion equations where the convergence length (Figure 1) is a function of time. The non-dimensional convergence length is defined as $L^* = L/R_0$ and corresponds to the non-dimensional axial distance at which $R^*(L^*, \tau)=0$.

Equation (9) was solved by means of the finite difference methods described in the next two subsections.

Non-adaptive method

Equation (9) can be written as

$$\frac{\partial \mathbf{U}}{\partial \tau}+\mathbf{H}\frac{\partial \mathbf{U}}{\partial z^*}=\mathbf{G}, \tag{16}$$

where $\mathbf{H} = \partial \mathbf{F}/\partial \mathbf{U}$ is a 4×4 Jacobian matrix whose eigenvalue $\lambda = M^*/m^*$ has an algebraic multiplicity of four and a geometric multiplicity of one. Therefore a similarity transformation of $\mathbf{H}$ yields a Jordan canonical form which has λ in the main diagonal and ones in the diagonal above the main diagonal.[5]

Equation (6) was solved in a fixed grid by means of an implicit method which uses one-point backward differences in time and upwinding/donor cell differences for the convection terms $\mathbf{H}\partial \mathbf{U}/\partial z^*$. Note that since m^* and M^* are strictly positive, the eigenvalues of $\mathbf{H}$ are $\lambda > 0$.

The term $\mathbf{G}$ was discretized by means of central differences, and the finite difference form of equation (16) can be written as

$$-\mathbf{C}_i^{n+1}\mathbf{U}_{i-1}^{n+1}+(\mathbf{I}+\mathbf{C}_i^{n+1})\mathbf{U}_i^{n+1}=\Delta\tau\mathbf{G}_i^{n+1}+\mathbf{U}_i^n, \tag{17}$$

where $\Delta\tau$ is the time step, $\mathbf{I}$ is the unit or identity matrix, the superscript n denotes the nth time level, i.e. $\tau^n = n\Delta\tau$, and

$$\mathbf{C}=\mathbf{H}\Delta\tau/\Delta z^*. \tag{18}$$

The overall accuracy of equation (17) is $O(\Delta\tau, \Delta z^*)$, and equation (17) represents a block bidiagonal system which can be solved by forward substitution in the following block iterative manner. The value of $\mathbf{U}^{n+1}$ was guessed and used to evaluate $\mathbf{G}_i^{n+1}$. Equation (17) was then solved and the procedure was repeated until

$$\left(\sum_{i=1}^{N_P}(\mathbf{U}_i^{*k+1}-\mathbf{U}_i^{*k})^2\right)^{1/2}\leqslant 10^{-4} \tag{19}$$

where N_P denotes the number of grid points and the superscript k denotes the kth iteration within the time step. Note that

$$(\mathbf{U}_i^{*k+1}-\mathbf{U}_i^{*k})^2=(\mathbf{U}_i^{*k+1}-\mathbf{U}_i^{*k})^{\mathrm{T}}(\mathbf{U}_i^{*k+1}-\mathbf{U}_i^{*k}).$$

At the nozzle exit, i.e. $i=1$, and at the convergence point, i.e. $i = N_C$, the first- and second-order derivatives which appear in $\mathbf{G}$ (equation (16)) were evaluated as

$$R_1^{*\prime}=(R_2^*-R_1^*)/\Delta z^*, \qquad R_1^{*\prime\prime}=(R_2^*-R_1^*)/\Delta z^{*2},$$

and

$$R_{N_C}^{*\prime}=(R_{N_C}^*-R_{N_C-1}^*)/\Delta z^* \qquad R_{N_C}^{*\prime\prime}=(R_{N_C}^*-R_{N_C-1}^*)/\Delta z^{*2},$$

i.e. forward and backward differences were used to evaluate $R^{*\prime}$ at the nozzle exit and at the convergence point respectively.

The main advantage of equation (17) is its simplicity. However, since the convection terms have been discretized by means of upwind differences, numerical diffusion is present in the calculations. Furthermore, since the solution of equation (17) was obtained in a fixed (non-adaptive) grid and the computations were performed in the interval $0 \leqslant z^* \leqslant L^*(\tau)$, where $L^*(\tau)$ is to be determined from the condition $R^*(L^*, \tau)=0$, i.e. L^* is not known, a sufficient number of grid points had to be placed to accurately account for the time dependence of the convergence length. This resulted in some grid points which were never used in the calculations, i.e. those for which $z^* > L^*(\tau)$.

In general, L^* does not coincide with a grid point. In the calculations presented in this paper, L^* was determined by linear interpolation as follows. Let $R^*_{N_c} > 0$ and $R^*_{N_c+1} < 0$, then

$$L^*=(z^*_{N_c+1} R^*_{N_c} - z^*_{N_c} R^*_{N_c+1})/(R^*_{N_c}-R^*_{N_c+1}).$$

The number of grid points used in the z^*-direction was varied from 300 to 400 and the axial step size was calculated on the basis of the maximum convergence length L^*_{max} as

$$\Delta z^* = L^*_{max}/(N_p-1), \tag{20}$$

where L^*_{max} is the steady state convergence length of the membrane corresponding to the largest value of the pressure coefficient C_{pn} used in the calculations.

The value of L^*_{max} was determined by solving equation (17) for the largest pressure coefficient used in the calculations until the following criterion for steady state was reached:

$$\left[\sum_{i=1}^{N_r}\left(\frac{\mathbf{U}_i^{*n+1}-\mathbf{U}_i^{*n}}{\Delta\tau}\right)^2\right]^{1/2} \leqslant 10^{-4}. \tag{21}$$

For both the steady state and transient analysis the convergence length was defined as the axial distance at which

$$|R^*| \leqslant 10^{-4}. \tag{22}$$

The above discussion clearly illustrates that since $L^* = L^*(\tau)$, the spatial step size Δz^* must first be determined from the steady solution of equation (17) corresponding to the largest value of the pressure coefficient C_{pn}. It also shows that for dynamic calculations in which $L^*(\tau) < L^*_{max}$, the grid points located in the interval $L^*(\tau) \leqslant z^* \leqslant L^*_{max}$ are never used in the calculations. This 'waste' of grid points is a consequence of the use of non-adaptive (fixed) grids for the solution of equation (9). Adaptive grids which do not 'waste' grid points will be presented in Part II.

The time step $\Delta\tau$ used in the calculations was equal to Δz^* for the steady state calculations which yield the value of L^*_{max}. The transient calculations reported in the next section were performed with $\Delta\tau=0{\cdot}01$.

Extensive calculations were performed to analyse the effects of $\Delta\tau$ and Δz^* on the numerical results. These calculations revealed that the values of $\Delta\tau=0{\cdot}01$ and Δz^* defined by equation (20) yield grid-independent results.

Lagrangian–Eulerian method

The non-adaptive finite difference method presented in the previous subsection introduces numerical diffusion because of the upwind discretization of the convection terms. In order to reduce the numerical diffusion errors, the mixed convection–diffusion system represented by

equation (9) was first written as

$$\frac{\partial m^*}{\partial \tau}+u^*\frac{\partial m^*}{\partial z^*}=-m^*\frac{\partial u^*}{\partial z^*}, \tag{23}$$

$$\frac{\partial u^*}{\partial \tau}+u^*\frac{\partial u^*}{\partial z}=Fr-\frac{1}{Nm^*}(C_{pn}R^*R^{*\prime}-J^{*\prime}), \tag{24}$$

$$\frac{\partial v^*}{\partial \tau}+u^*\frac{\partial v^*}{\partial z^*}=\frac{1}{m^*N}\left(-\frac{J^{*\prime}}{R^{*\prime}}+C_{pn}R^*\right), \tag{25}$$

$$\frac{\partial R^*}{\partial \tau}+u^*\frac{\partial R^*}{\partial z^*}=v^*. \tag{26}$$

The mixed convection–diffusion operators of equations (23)–(26) were split into the following sequence of operators:

$$L_C:\quad \frac{\partial \mathbf{V}^*}{\partial \tau}+u^*\frac{\partial \mathbf{V}^*}{\partial z^*}=0, \tag{27}$$

$$L_D:\quad \frac{\partial \mathbf{V}^*}{\partial \tau}=\mathbf{Q}^*, \tag{28}$$

where

$$\mathbf{V}^*=(m^*, u^*, v^*, R^*)^T, \tag{29}$$

$$\mathbf{Q}^*=\left[-m^*\frac{\partial u^*}{\partial z^*}, Fr-\frac{1}{Nm^*}(C_{pn}R^*R^{*\prime}-J^{*\prime}), \frac{1}{m^*N}\left(-\frac{J^{*\prime}}{R^{*\prime}}+C_{pn}R^*\right), v^*\right]^T. \tag{30}$$

The convection operator of equation (27) was solved by means of the method of characteristics, which yields

$$\mathbf{V}^*=\mathbf{D}, \tag{31}$$

where $\mathbf{D}$ is a constant vector, i.e. $\mathbf{V}^*$ is constant along the characteristic lines $dz^*/d\tau=u^*$.

Note that according to equation (27) and the second component of the vector $\mathbf{V}^*$, u^* is constant along the characterisitic lines. Therefore the slope of these lines is constant and

$$z_c^*-z^{*n}=\Delta\tau_C u^{*n}, \tag{32}$$

where $\Delta\tau_C$ denotes the (non-dimensional) time step used to solve the convection operator and z_c^* is the location of a point at $\tau_C=\tau^n+\Delta\tau_C$ which was at z^{*n} at τ^n.

The locations z_c^* of the method of characteristics do not in general coincide with those of the (fixed) grid points z_i^*, $i=1, 2, \ldots, N_P$, used to solve equation (28). Therefore the solution $\mathbf{V}^*$ of the convection operator must be interpolated onto the Eulerian grid used to solve the operator L_D. In the calculations presented in this paper, cubic splines were used to interpolate the results of the convection operator onto the fixed Eulerian grid, and the operator L_D was solved by means of one-point backward differences for the time derivatives and central differences for the spatial derivatives in an analogous manner to equation (17).

Although the method of characteristics used to solve the convection operator eliminates the numerical diffusion which would be introduced if this operator were solved in a fixed grid, the results of the Lagrangian–Eulerian method presented in this section may exhibit numerical diffusion errors and/or oscillations owing to the interpolation of the results of the convection

operator onto the (fixed) Eulerian grid used to solve the operator L_D. Furthermore, since the operator L_D is solved in a non-adaptive grid, some grid points may not be used in the calculations as indicated in the previous subsection.

In the calculations presented in this paper $\tau_C = \tau_D = \Delta\tau/2$, where $\Delta\tau$ is the time step, i.e. $\Delta\tau = \tau^{n+1} - \tau^n$, and $\Delta\tau_D$ is the time step used to solve the operator L_D. The value of Δz^* was the same as that of the previous section.

PRESENTATION OF RESULTS

We consider liquid membranes in steady state with $C_{pn} = 0$ and subject them at $\tau > 0^+$ to the pressure coefficients shown in Figure 2, i.e. we study the dynamic response of liquid membranes to positive and negative step and ramp changes in the pressure coefficient. The response of liquid membranes to these changes in the pressure coefficient will help us to understand the membrane response to the pressure coefficients to be reported in Part II.

In Figure 2, τ denotes the non-dimensional time measured from the instant at which the pressure change is introduced, i.e. from steady state, C_{pna} denotes the maximum/minimum amplitude of the pressure change and t_d is the time during which C_{pn} varies linearly with τ.

The calculations presented in this section were performed until $\tau = 20$; the values of the parameters used in the calculations are shown in Table I, and in all the figures the non-dimensional convergence length has been normalized with respect to the dimensionless convergence length corresponding to steady state and $C_{pn} = 0$, i.e. with respect to L_{ss}^*.

In order to obtain a clear picture of the results presented in Figures 3–20, it is convenient to define the response and lag times.

The response time is defined as the difference between the time at which the change in the pressure coefficient is imposed, i.e. $\tau = 0$, and the time at which the convergence length changes by more than 3%. The response time is a direct measure of the inertia of the membrane.

The lag time is defined as the difference between the time at which the C_{pn} curve reaches its extremum and the time at which the convergence length curve reaches its corresponding

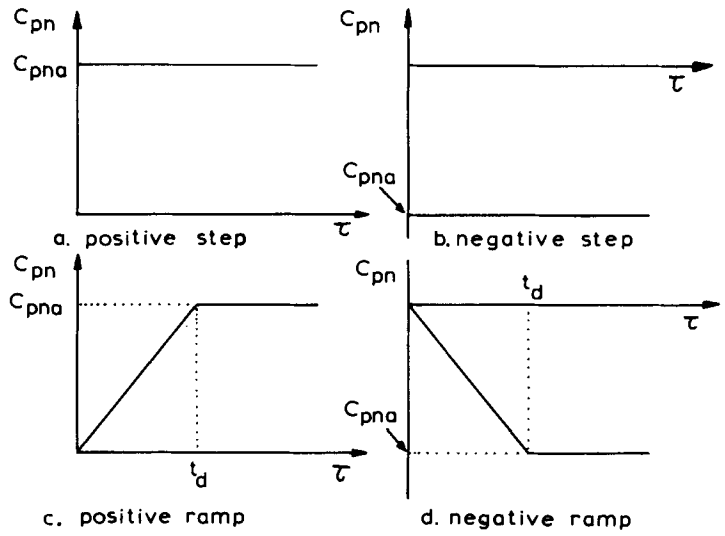

Figure 2. Types of variations of C_{pn} used in the analysis

Table I. Values of the parameters used in the calculations

Figure	Fr	N	θ_0 (deg)	C_{pna}	t_d	Type of variation of C_{pn}
3	Variable	15	0	0·5	0	Positive step
4	1	Variable	0	0·5	0	Positive step
5	1	15	Variable	0·1	0	Positive step
6	1	15	0	Variable	0	Positive step
7	Variable	15	0	−0·5	0	Negative step
8	1	Variable	0	−0·5	0	Negative step
9	1	15	Variable	−0·5	0	Negative step
10	1	15	0	Variable	0	Negative step
11	1	15	0	0·5	Variable	Positive ramp
12	Variable	15	0	0·5	10	Positive ramp
13	1	Variable	0	0·5	10	Positive ramp
14	1	15	Variable	0·1	10	Positive ramp
15	1	15	0	Variable	10	Positive ramp
16	1	15	0	−0·5	Variable	Negative ramp
17	Variable	15	0	−0·5	10	Negative ramp
18	1	Variable	0	−0·5	10	Negative ramp
19	1	15	Variable	−0·5	10	Negative ramp
20	1	15	0	Variable	10	Negative ramp

extremum. The lag time is an indication of how closely the liquid membrane is able to follow the changes in the pressure coefficient.

Membrane response to a positive step

Figures 3–5 show the response of membranes to a fixed positive step change in C_{pn}. In Figure 3 the parameter that is varied is the Froude number. It is known from analytical studies[1] that the convergence length varies almost linearly with the Froude number when the other membrane parameters are fixed. This can be written mathematically as

$$L^* = k_1(C_{pn}(\tau), N, \theta_0)Fr, \tag{33}$$

where k_1 is a constant of proportionality which depends on C_{pn}, N and θ_0. The steady state convergence length L_{ss}^* corresponding to $C_{pn} = 0$ can similarly be expressed as

$$L_{ss}^* = k_2(C_{pn} = 0, N, \theta_0)Fr, \tag{34}$$

where k_2 is the proportionality constant corresponding to $C_{pn} = 0$. From equations (33) and (34) it follows that

$$L^*/L_{ss}^* = k_1(C_{pn}(\tau), N, \theta_0)/k_2(C_{pn} = 0, N, \theta_0) = k_3(\tau, N, \theta_0), \tag{35}$$

where k_3 does not depend on Fr. Since N and θ_0 are fixed, k_3 is a function of τ only. This is evident from Figure 3 where the responses of the membrane for all Froude numbers fall into one curve.

The response of a membrane for different convergence parameters is shown in Figure 4. It may be recalled that the convergence parameter is a measure of the magnitude of inertial forces relative to the magnitude of surface tension (equation (7)). The smaller the value of N, the lesser is the inertia of the membrane and the quicker is the membrane response. Conversely, for high values of N the membrane response is sluggish. The membrane response and lag times increase with increasing N, and in the limit $N \to \infty$ (zero surface tension) the response and lag times tend

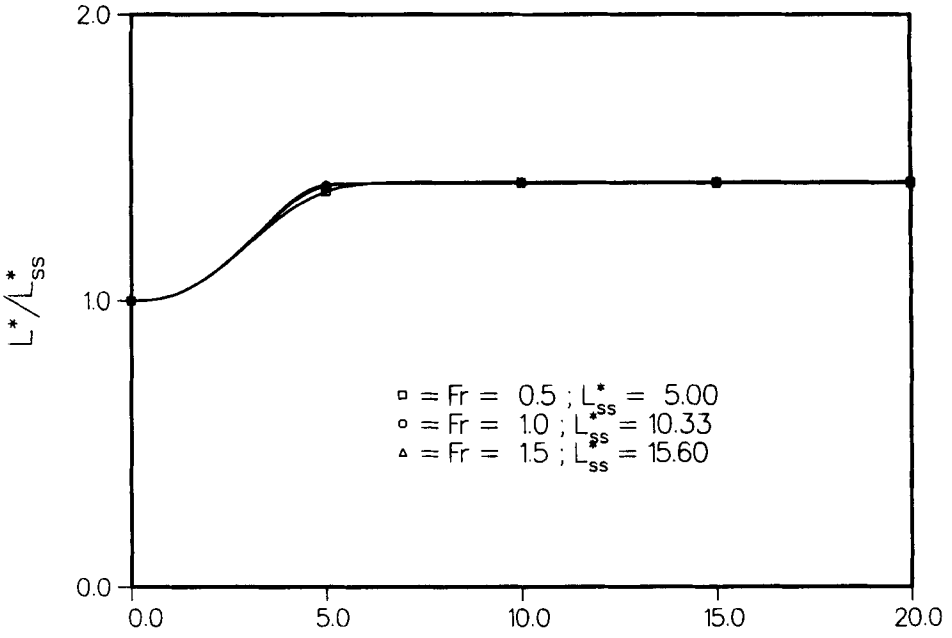

Figure 3. Normalized dimensionless convergence length as a function of the Froude number for a positive step change in C_{pn}

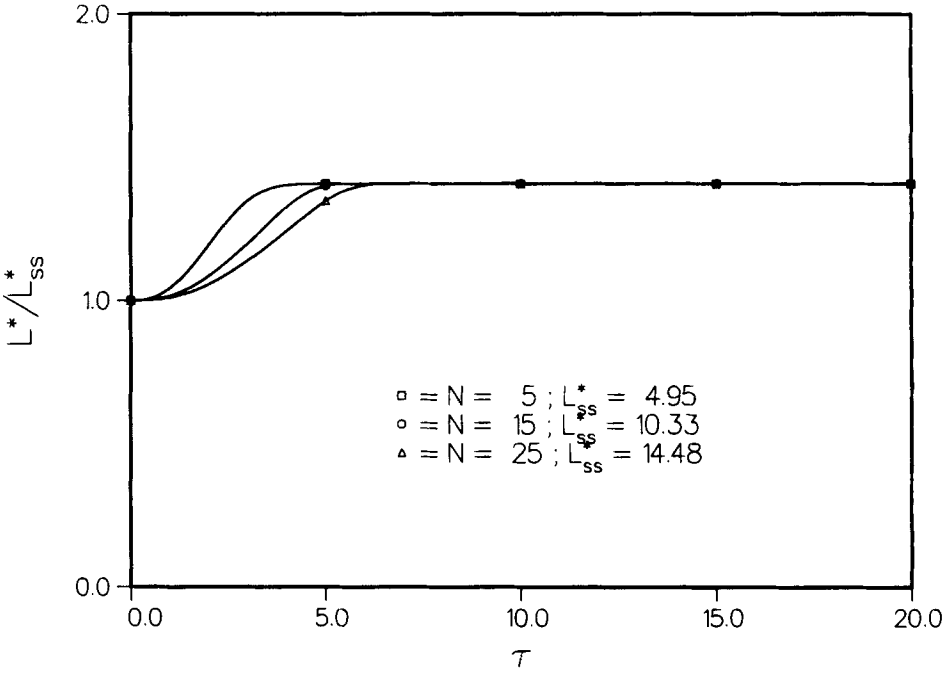

Figure 4. Normalized dimensionless convergence length as a function of the convergence parameter for a positive step change in C_{pn}

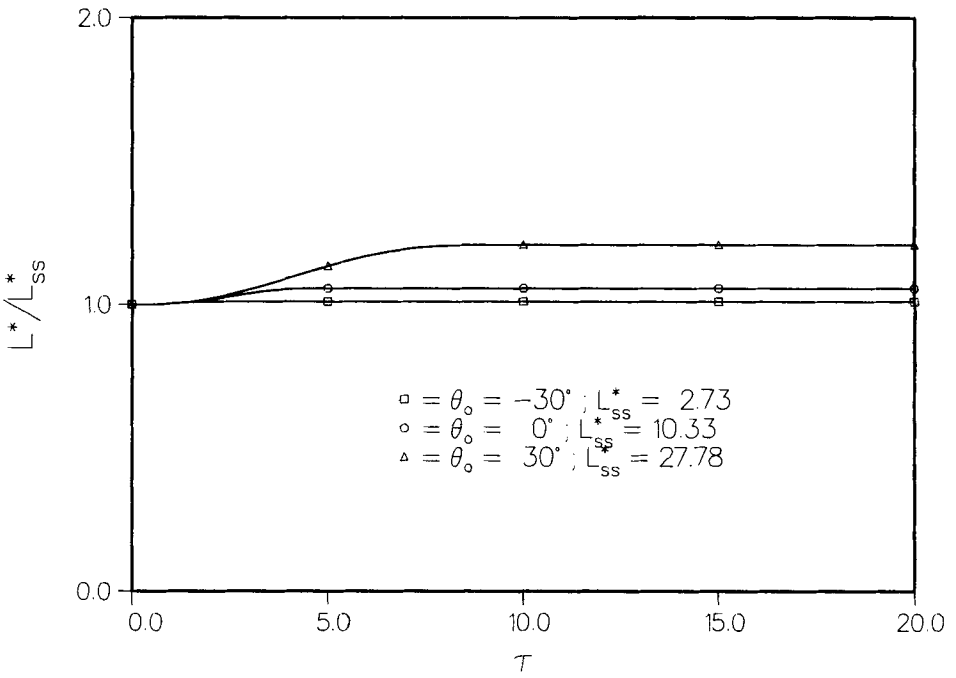

Figure 5. Normalized dimensionless convergence length as a function of the nozzle exit angle for a positive step change in C_{pn}

to infinity. For example, in Figure 4 the response time for $N = 25$ is about 0·5 while the response times for $N = 15$ and 25 are about 0·9 and 1·2 respectively, and the lag times for $N = 5$, 15 and 25 are approximately 4·0, 5·0 and 6·0 respectively.

It can be seen from Figure 5 that as the nozzle exit angle θ_0 increases, the response of the membrane increases. For large values of the nozzle exit angle the pressure difference across the membrane acts over a greater surface area and hence the membrane response is faster. For membranes with small θ_0 the converse is true and the response is sluggish.

The influence of the magnitude of the step variation on the pressure coefficient, namely C_{pna}, is presented in Figure 6. In this figure the membrane parameters N, Fr and θ_0 are kept constant. For large C_{pna} the driving force in the form of the pressure difference is high and so is the convergence length of the membrane. As C_{pna} decreases, the driving force drops and the convergence length decreases.

Membrane response to a negative step

In Figures 7–10 a negative step change in C_{pn} is imposed on the liquid membrane and the influence of the membrane parameters on the response of the membrane is studied. Negative values of C_{pn} indicate that the membrane is pressurized from outside, i.e. $p_e > p_i$. The behaviour of the membrane is similar to those described in Figures 3–6 with the following distinctions: (i) the convergence length decreases from its steady state value in response to the pressurization from outside the membrane; (ii) the response time and the lag time are much smaller than those for positive changes in C_{pn}.

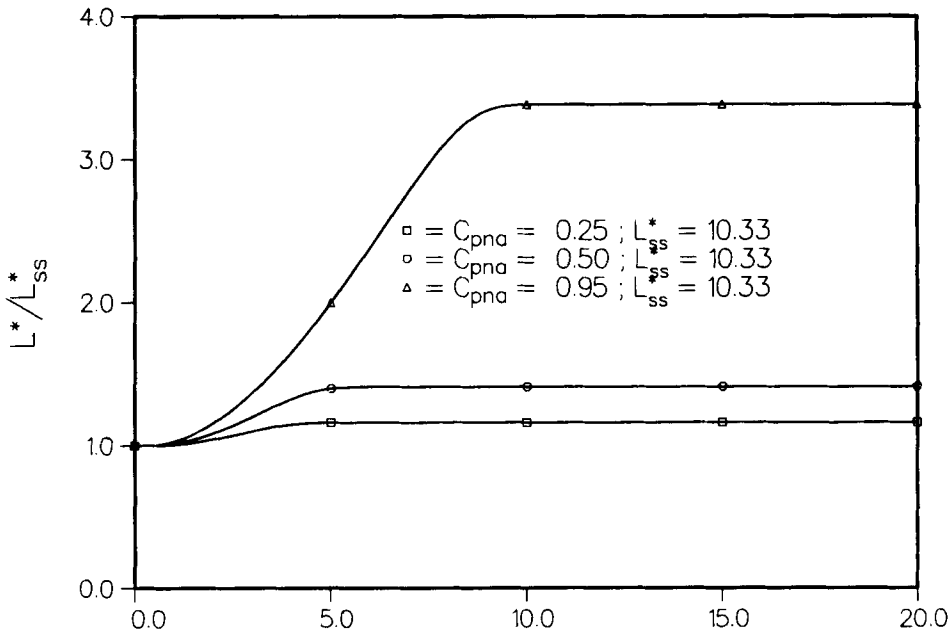

Figure 6. Normalized dimensionless convergence length as a function of C_{pna} for a positive step change in C_{pn}

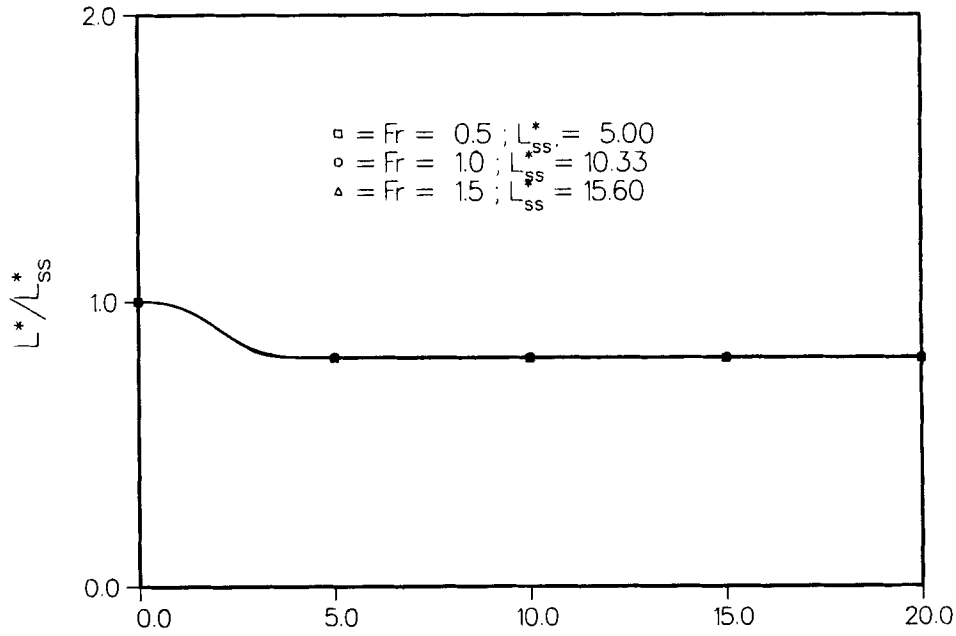

Figure 7. Normalized dimensionless convergence length as a function of the Froude number for a negative step change in C_{pn}

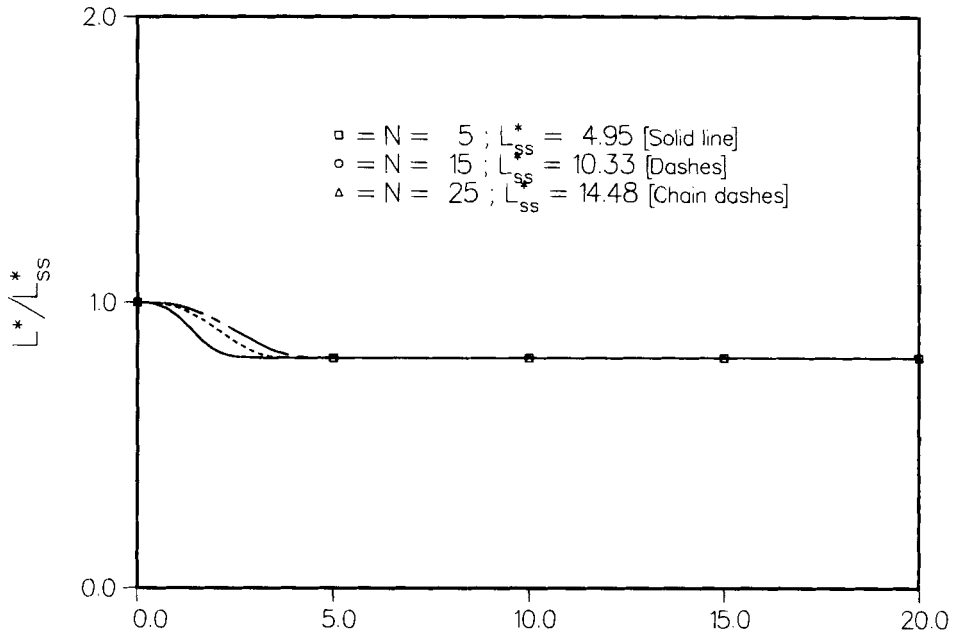

Figure 8. Normalized dimensionless convergence length as a function of the convergence parameter for a negative step change in C_{pn}

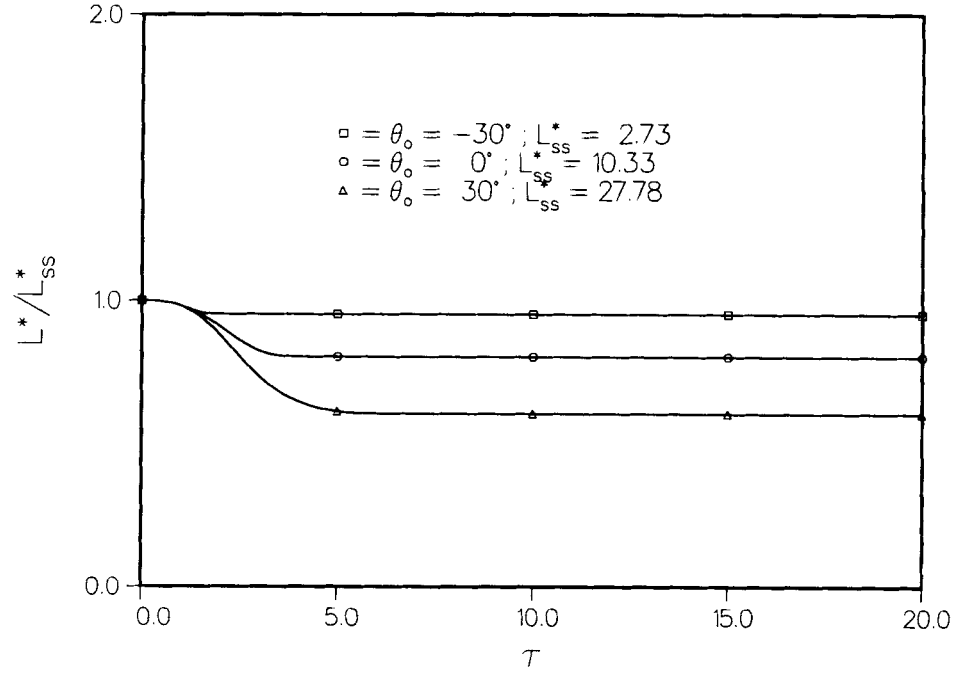

Figure 9. Normalized dimensionless convergence length as a function of the nozzle exit angle for a negative step change in C_{pn}

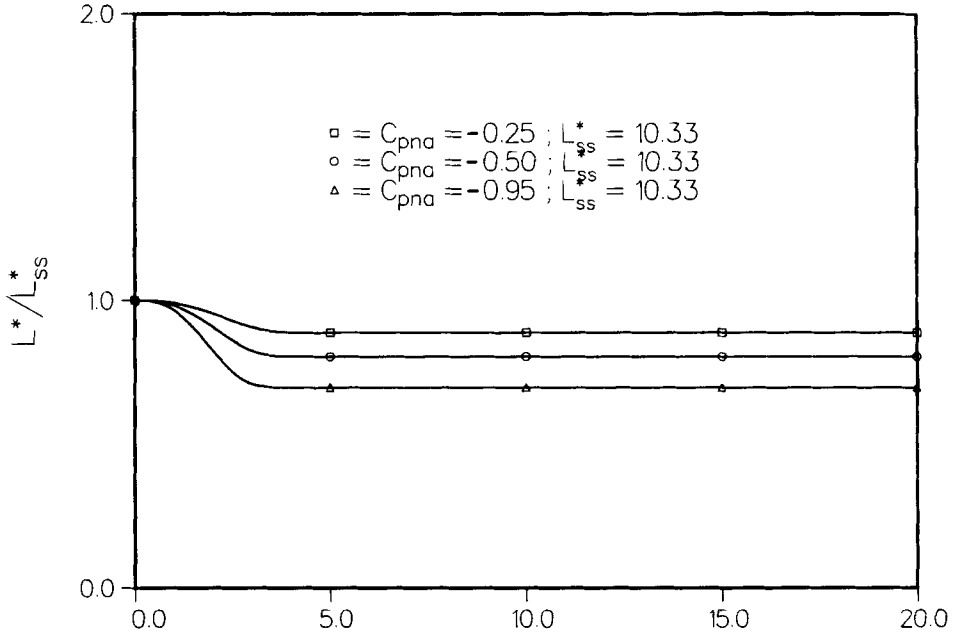

Figure 10. Normalized dimensionless convergence length as a function of C_{pna} for a negative step change in C_{pn}

Membrane response to a positive ramp

Figure 11 shows the response of a membrane to positive ramp changes in the pressure coefficient. The parameter that is under consideration here is the rate of change of the pressure coefficient measured by t_d. The response time increases and the lag time decreases as t_d increases. This phenomenon can be explained as follows. A high value of t_d implies that the membrane is pressurized slowly and it takes a longer time for the pressure difference to overcome the inertia of the membrane; consequently, the response time is higher. It is also true that once the inertia is overcome, the membrane responds rapidly to changes in the pressure coefficient. Thus for large values of t_d the relatively fast response of the membrane enables it to catch up with the change in C_{pn}, thereby reducing the lag time. In the limit $t_d \to \infty$ the response time tends to infinity and the lag time tends to zero.

Figures 12–15 illustrate the influence of positive ramp changes in the pressure cofficient on the membrane response. These figures indicate that the membrane response follows closely that observed for positive step chages in C_{pn}.

Membrane response to a negative ramp

The variations of the normalized convergence length in response to negative ramp changes in C_{pn} are shown in Figures 16–20. The behaviour observed in Figures 11–15 for positive ramp changes is exhibited in these figures also.

The results presented in Figures 3–20 were obtained by means of the two non-adaptive methods presented in the previous section. These methods yielded almost identical results; the differences were less than 1% when $\tau_C = \tau_D = \Delta\tau/2$. The Lagrangian–Eulerian method yielded some overshoots and undershoots near $\tau = 0^+$ for the positive and negative step changes in the

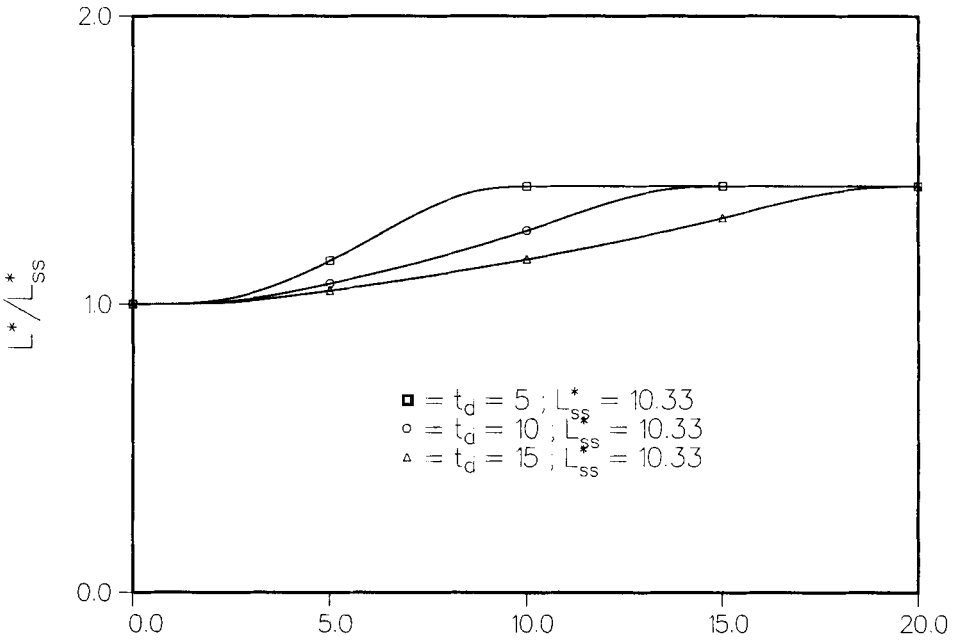

Figure 11. Normalized dimensionless convergence length as a function of t_d for a positive ramp change in C_{pn}

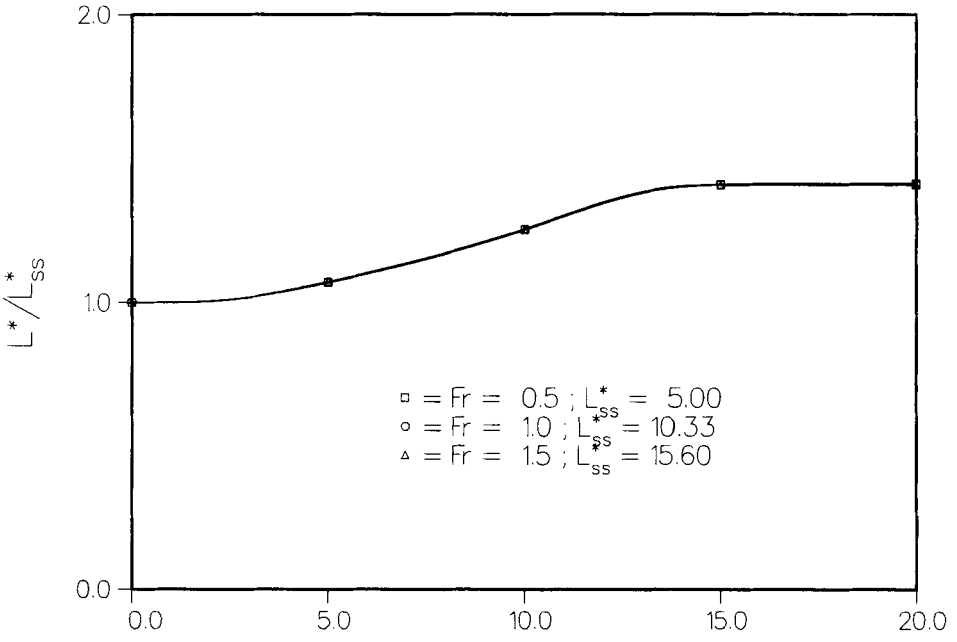

Figure 12. Normalized dimensionless convergence length as a function of the Froude number for a positive ramp change in C_{pn}

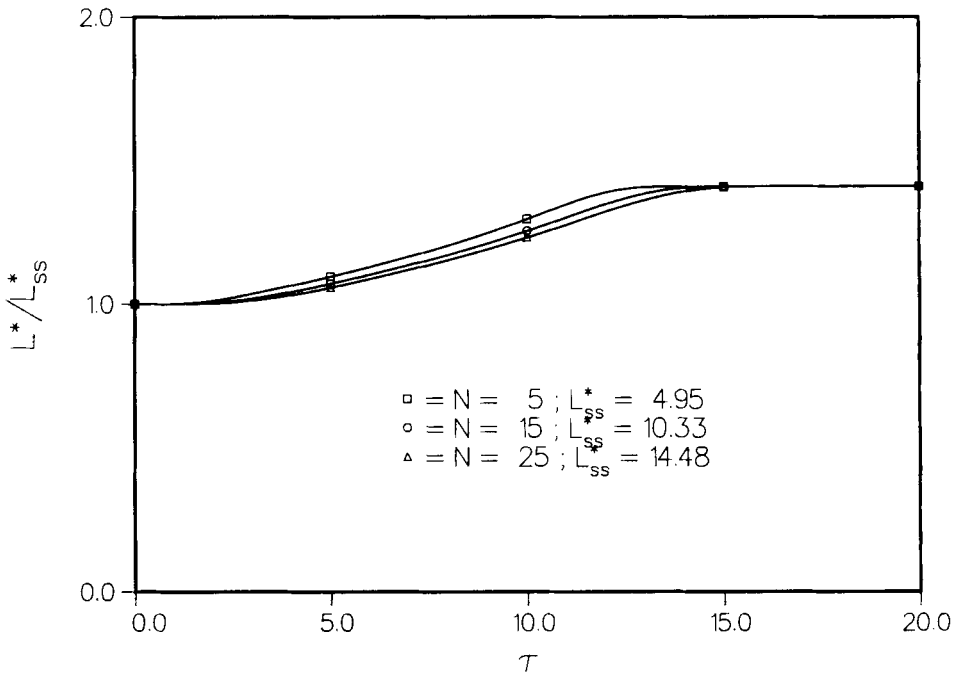

Figure 13. Normalized dimensionless convergence length as a function of the convergence parameter for a positive ramp change in C_{pn}

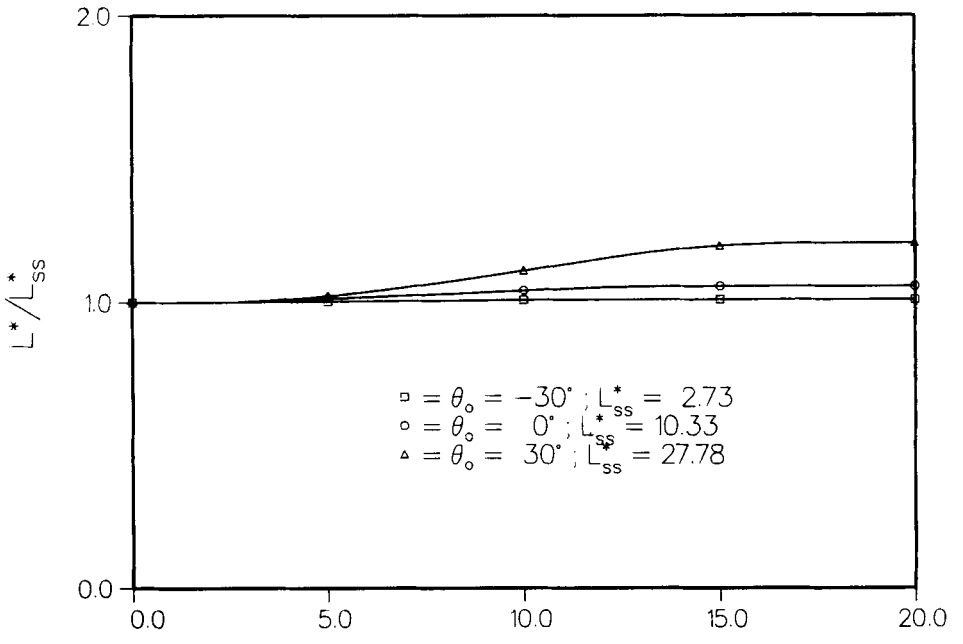

Figure 14. Normalized dimensionless convergence length as a function of the nozzle exit angle for a positive ramp change in C_{pn}

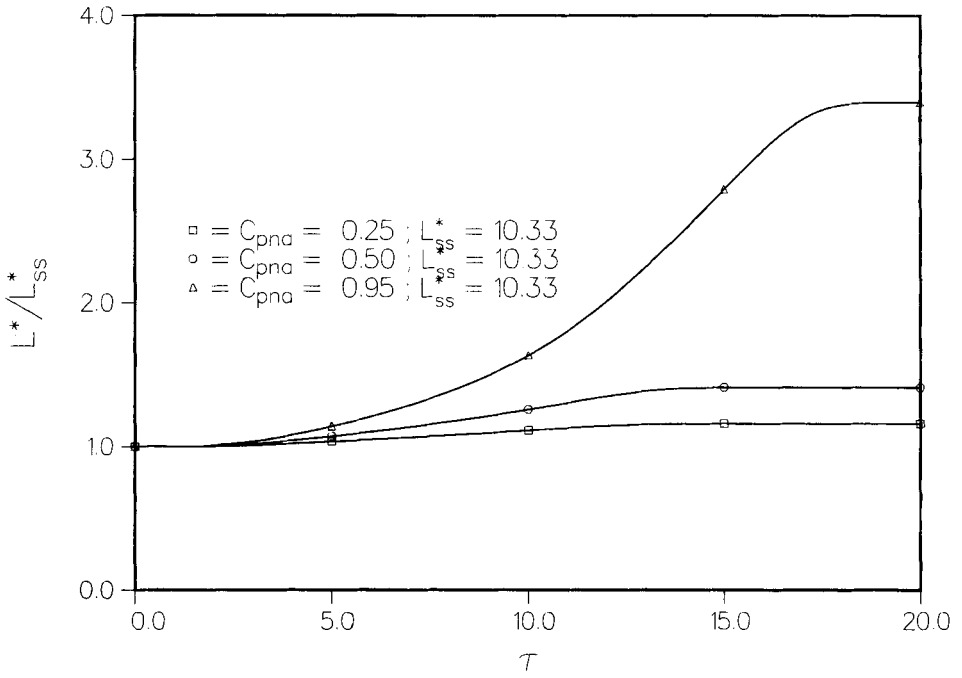

Figure 15. Normalized dimensionless convergence length as a function of C_{pna} for a positive ramp change in C_{pn}

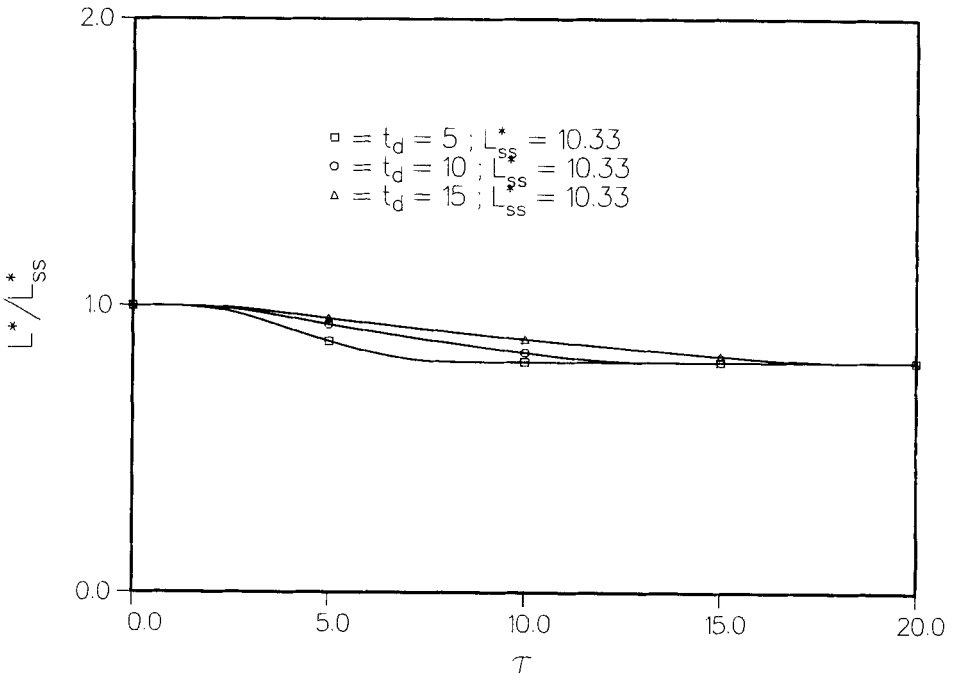

Figure 16. Normalized dimensionless convergence length as a function of t_d for a negative ramp change in C_{pn}

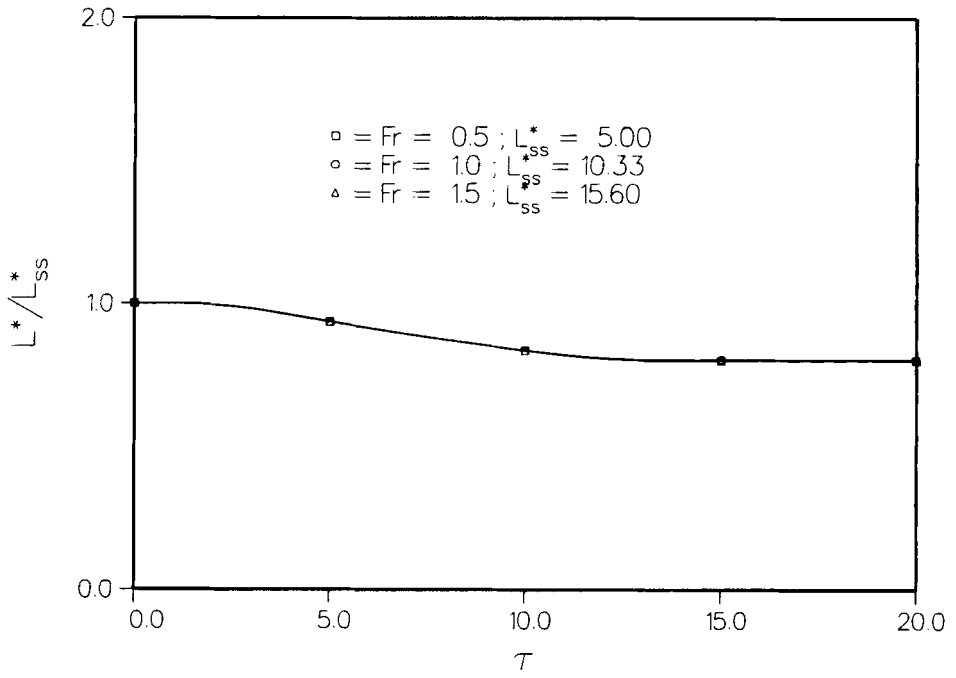

Figure 17. Normalized dimensionless convergence length as a function of the Froude number for a negative ramp change in C_{pn}

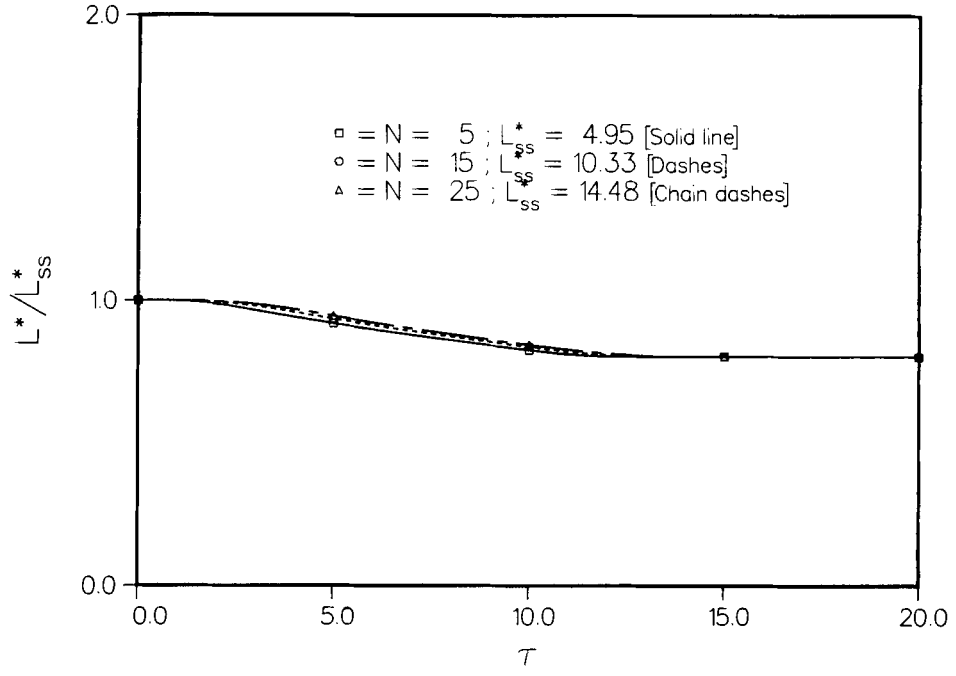

Figure 18. Normalized dimensionless convergence length as a function of the convergence parameter for a negative ramp change in C_{pn}

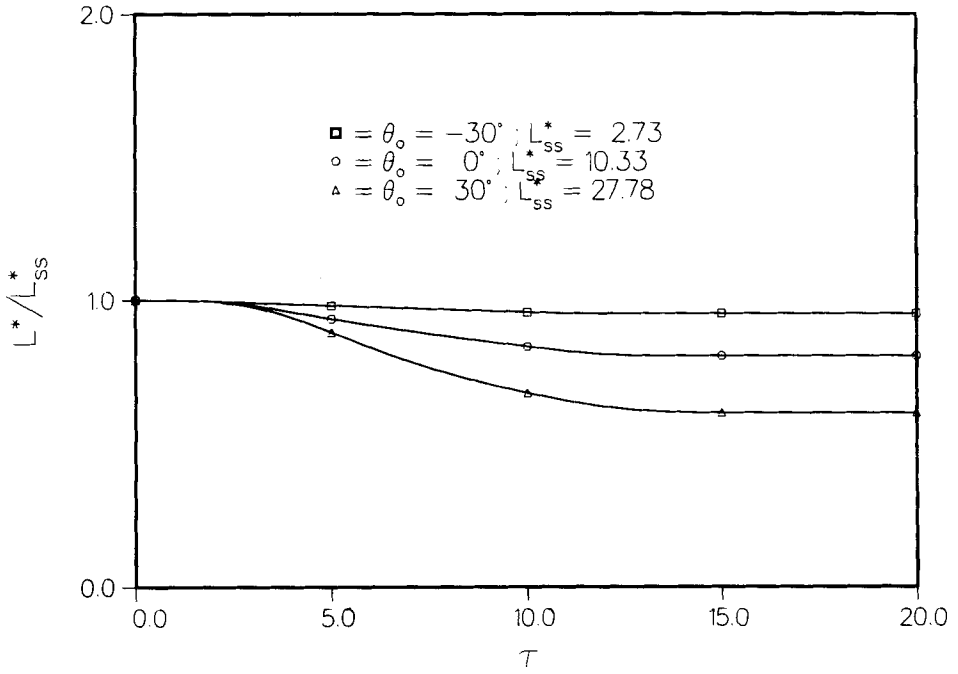

Figure 19. Normalized dimensionless convergence length as a function of the nozzle exit angle for a negative ramp change in C_{pn}

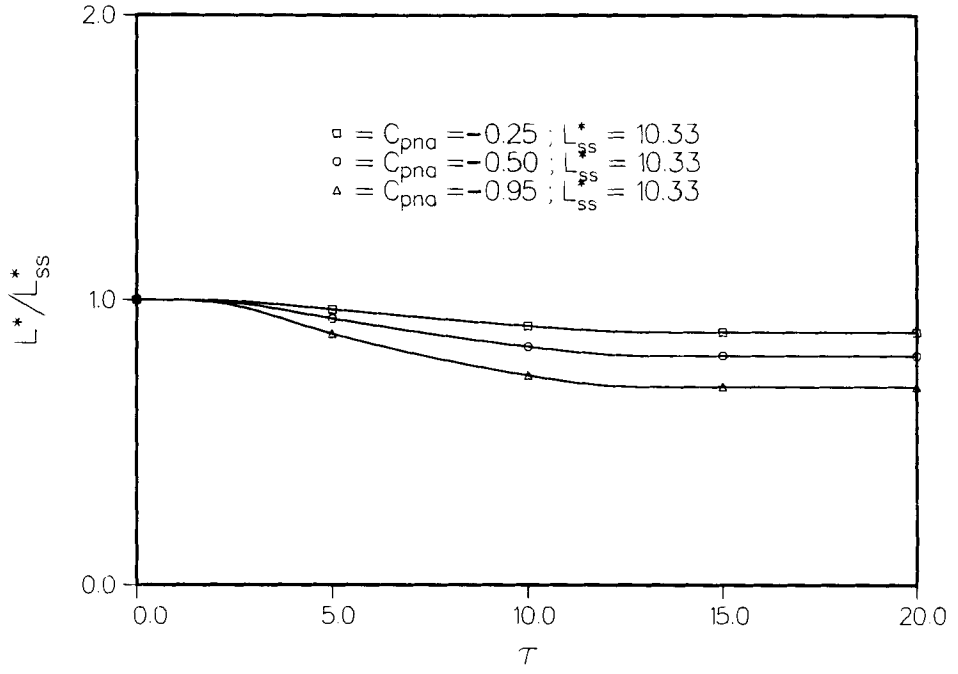

Figure 20. Normalized dimensionless convergence length as a function of C_{pna} for a negative ramp change in C_{pn}

pressure coefficient. These overshoots and undershoots were a consequence of the interpolation of the results of the convection operator onto the fixed Eulerian grid used to solve the operator L_D and can be reduced, but not eliminated, by reducing the time step.

The Lagrangian–Eulerian method did not preserve mass and linear momentum exactly. This was also attributed to the interpolation, which should be monotone and positivity-preserving and must satisfy the conservation principles of mass and linear momentum in the present application.

Except in the cases where steep pressure changes were imposed, both the non-adaptive and Lagrangian–Eulerian finite difference methods presented in this paper produced almost identical (within 1%) numerical results. However, since these methods use fixed grids, the grid points located in the interval $L^*(\tau) \leqslant z^* \leqslant L^*_{max}$ were never used in the calculations and the value of L^*_{max} had to be determined before the transient calculations were performed. The adaptive finite difference methods presented in Part II do not use unnecessary grid points and do not require the determination of L^*_{max}.

CONCLUSIONS

The time-dependent equations governing the dynamics of inviscid, isothermal, axisymmetric membranes have been solved numerically by means of non-adaptive and Lagrangian–Eulerian finite difference methods, and the membrane response was determined as a function of the Froude number, convergence parameter and nozzle exit angle for positive and negative step and ramp changes in the pressure coefficient.

The results indicate that the response time, which is the time that the membrane takes to start responding noticeably to the changes in the pressure coefficient, is directly dependent on the inertia of the membrane. Response times are higher for small values of the convergence parameter and small values of θ_0. For step and ramp changes in C_{pn} the quantity L^*/L^*_{ss} is independent of the Froude number. This is because the convergence length is linearly proportional to the Froude number and hence the Froude number drops out of the ratio L^*/L^*_{ss}. The response of membranes to negative step and negative ramp changes are similar to the response to positive step and positive ramp changes respectively. However, the response is quicker for negative changes. In other words, the membrane response time decreases as the value of C_{pn} decreases.

The non-adaptive and Lagrangian–Eulerian finite difference methods yield almost identical (within 1%) results when the time steps used to solve the convection and diffusion operators are equal to half the time step used in the non-adaptive method.

The non-adaptive method uses a fixed grid, upwind differences for the convection terms and a block iterative method for solving the governing mixed convection–diffusion system of equations. However, the upwinding of the convection terms introduces numerical diffusion errors.

The Lagrangian–Eulerian technique uses operator splitting and decomposes the mixed convection–diffusion operator into a sequence of convection and diffusion problems. The convection operator is solved exactly by means of the method of characteristics and its results are interpolated onto the fixed (Eulerian) grid used to solve the diffusion operator. Although the exact solution of the convection operator eliminates the numerical diffusion errors which would be produced if this operator were solved in a fixed grid, the interpolation yields overshoots and undershoots where steep flow gradients exist or when steep changes in the pressure coefficient are imposed. Such an interpolation should also preserve the monotonicity and positivity of the solution and ensure mass and linear momentum conservation.

Since both the non-adaptive and Eulerian–Lagrangian finite difference procedures presented in this paper use fixed (non-adaptive) grids, it is first necessary to obtain an estimate of the

(unknown) length of the computational domain; this requires that the largest steady state convergence length be determined before the transient (dynamic) calculations are performed. Furthermore, since the transient convergence length is smaller than the maximum steady state convergence length, some grid points are never used in the calculations. This limitation is eliminated in Part II where solution-adaptive methods for the dynamics of liquid membranes are presented.

ACKNOWLEDGEMENTS

This work was supported by the Office of Basic Energy Sciences, U.S. Department of Energy under Grant No. DE-FG02-86ER13597 with Dr. Oscar P. Manley as the technical monitor. This support is greatly appreciated. The authors also wish to acknowledge the support provided by CRAY Research, Inc. through a grant from the 1988 CRAY Research and Development Grant Program and by the Pittsburgh Supercomputing Center.

REFERENCES

1. J. I. Ramos, 'Liquid curtains: I. Fluid mechanics', *Chem. Eng. Sci.*, **43**, 3171–3184 (1988).
2. J. I. Ramos, 'Liquid membranes: formulation and steady state analysis', *Report CO/89/4*, Department of Mechanical Engineering, Carnegie-Mellon University, Pittsburgh, PA, 1989.
3. J. I. Ramos and R. Pitchumani, 'Unsteady response of liquid curtains to time-dependent pressure oscillations', *Report CO/88/4*, Department of Mechanical Engineering, Carnegie-Mellon University, Pittsburgh, PA, 1988.
4. J. I. Ramos and R. Pitchumani, 'Unsteady response of liquid membranes to time-dependent pressure oscillations', *Report CO/89/3*, Department of Mechanical Engineering, Carnegie-Mellon University, Pittsburgh, PA, 1989.
5. G. E. Shilov, *Linear Algebra*, Dover, New York, 1977, pp. 112–113.